

Mixing enthalpy of Ag–Sn system at 1150 °C

Ksenia Oleinik¹ · Andrey Bykov¹ · Eduard Pastukhov¹

Received: 3 August 2017 / Accepted: 12 November 2017 / Published online: 20 November 2017
© Akadémiai Kiadó, Budapest, Hungary 2017

Abstract This paper presents thermodynamic results of Ag–Sn alloys mixing at 1150 °C. The need for binary data on mixing enthalpy ΔH_{mix} appeared obvious in the process of calorimetric study of the ternary system Ag–Cu–Sn known as the promising lead-free solder. The mixing enthalpies of Ag–Sn system were measured by drop calorimetry method using SETARAM MHTC thermal analyzer. All the tests were conducted in the dynamic protective atmosphere of argon. The calorimeter's sensitivity calibration was performed with the use of pure metals (Ag, Sn) and standard leucosapphire samples and consisted of two stages. The use of two-stage calibration procedure improves significantly the convergence of two branches of ΔH_{mix} isotherm plotted from the pure component toward each other. The experimental results were approximated with analytical function using quasi-chemical modification of subregular solutions model (quasi-chemical model of Sharkey et al.) postulating the presence of both pair and triple interactions in solution. The resultant equation is $\Delta H_{\text{mix}} = N_{\text{Ag}} \cdot N_{\text{Sn}} (-27.7075 \cdot N_{\text{Ag}} - 0.9977 \cdot N_{\text{Sn}} + 27.7079 \cdot N_{\text{Ag}} \cdot N_{\text{Sn}})$, kJ mol⁻¹, where N is the component mole fraction. The measured compositional dependence of ΔH_{mix} is substantially asymmetric like the previous results of the other authors, but, in contrast to those results, it does not change the sign and is entirely negative in the whole range of concentrations.

Keywords Thermodynamic properties · Enthalpy increment · Drop calorimetry · Liquid alloy Ag–Sn · Subregular solution

Introduction

Sn–Pb solders were widely used for many years by electrical and electronic equipment (EEE) manufacturers as a joining material because of low cost, good wetting, easy melting and superior mechanical properties despite the well-known fact of toxic effect of Pb on human health and severe environment pollution [1, 2]. However, rapid advances in microelectronic design and technology in recent decades led to multiple accelerations of Pb-containing electronic waste (i.e., the used EEE) accumulation and made Pb pollution a major issue [3]. Beginning with the middle of the noughties, a number of legislations restricting the use and disposal of Pb–Sn solders (e.g., EU Directive 2002/95/EC) had been implemented in the different parts of the world [4]. Since that time, the process of gradual substitution of traditional soldering alloys with nonpolluting alternative materials was launched and a wide variety of Pb-free soldering compositions was developed [1, 4–12].

A binary and ternary alloys of Sn with Ag and/or Cu are recognized [6, 9, 13–15] as the most promising materials in this line, but some of their functional properties are inferior to those of conventional Pb-containing solders [2, 3, 13, 16, 17]. Ag–Sn (Ag–Cu–Sn) alloys are potential candidates for using as individual lead-free solders as well as the base of more complicated compositions. An improvement in these lead-free alloys may be achieved by adding a fourth alloying element (Mn, Ce, Ni, Ti, Co, Al, Fe, Bi, Sb, In or Au) [13, 16, 18, 19] or by reinforcing the

✉ Andrey Bykov
a.s.bykov54@mail.ru

¹ Institute of Metallurgy, Ural Branch of the Russian Academy of Sciences, 101 Amundsena Str, Yekaterinburg, Russia 620016

soldering material with carbon nanoparticles [20, 21]. In any case, the knowledge of the base alloys mixing enthalpies is essential for the further development of new high-performance solders by time- and labor-saving way.

Thermodynamics of the considered Ag–Sn system formation was studied earlier, and the data on mixing enthalpy ΔH_{mix} of liquid alloys Ag–Sn were reported by different authors [22–24]. The published results are in good qualitative agreement with each other. In all the cases, a distinct exothermic interaction of liquid components was observed within compositional range between 0 and 65–80 at.% Sn with the extremum $-2.7 \div -3.3 \text{ kJ mol}^{-1}$ at about 20 at.% Sn. For the rest compositions, a weak (less than 0.5 kJ mol^{-1}) endothermic interaction is typical. Meanwhile, the data presented by different authors have a quantitative discrepancy up to 0.5 kJ mol^{-1} , and it may be attributed to the lack of identical experimental conditions, temperatures in particular.

The present work is a part of a large-scale investigation of alloy formation in the ternary system Ag–Cu–Sn including boundary binary solutions Ag–Sn, Cu–Sn, Ag–Cu. To obtain the accurate results, it is critically important to measure all the involved compositions under the identical conditions. This is why we undertook one more independent attempt of Ag–Sn ΔH_{mix} calorimetric determination using the fixed local measuring parameters. Earlier the mixing enthalpies of liquid alloys Ag–Cu–Sn were measured by Luef et al. [5] at the temperatures not higher $900 \text{ }^\circ\text{C}$, i.e., in the limited compositional range. We carry out experiments at the elevated temperature $1150 \text{ }^\circ\text{C}$ above melting points of the pure components and hope much to get new information on Ag–Cu–Sn alloys mixing enthalpies, which will be a supplementary contribution to the existing thermodynamic databases such as the COST-Action 531 of the European Union.

Materials

The considered alloys were prepared from tin (99.999% purity) and silver (999.99% purity). All measurements were taken in a protective dynamic atmosphere of argon 5.0 (purity 99.999) with a flow rate of this gas of 10 ml min^{-1} . The instrument sensitivity calibration was taken using metal components of the alloy and standard samples of synthetic leucosapphire. The masses of metal and sapphire calibrating samples were 55–130 and 50–54 mg, respectively.

Experimental

The components were mixed by drop calorimetry in the experimental chamber of a SETARAM MHTC thermal

analyzer. The mixing enthalpy was measured as follows: First, pure metals were cut into the samples of approximately equiaxial shape and overall size not more than 4 mm and a mass within 43–152 mg. The latter were weighed on an analytical balance Sartorius CPA225D with an accuracy of $\pm 0.01 \text{ mg}$. Then, the metal pieces were loaded into the programmable introducing device for their subsequent feeding into the hot experimental chamber every 15 min. The main parameters of the experiment (initial and final temperatures, the duration and temperature of the isothermal exposures, the sequence of the gas circuit electromagnetic valves switching, etc.) were set with the use of Calisto 1.088 software.

After evacuating the air from the calorimeter down to the air pressure 2.5×10^{-2} torr and creating protective inert atmosphere in it, the prespecified sequence of the temperature stages of the experiment was started. The analytical signal of the heat flux, the sample temperature and the current time were recorded using the Calisto program with the formation of a data file on the computer's hard disk. Afterward, the recorded data were processed to determine the values of the enthalpy change following the introduction of each sample into a measuring detector heated to a predetermined temperature. A detailed premise of the procedure for determining the integral mixing enthalpy ΔH_{mix} by drop calorimetry is given in [25].

The reference values on pure metal component enthalpies that are necessary for the estimation of the calibration factor k were taken from [22, 26]. It was found out that the data on Ag in [22] and [26] at $1150 \text{ }^\circ\text{C}$ are practically the same. But this relationship is quite another matter concerning pure Sn. The difference between enthalpy values of Sn given by Dinsdale in [26] and by Kubaschewski and Alcock in [22] at a temperature $1150 \text{ }^\circ\text{C}$ is as much as 10%. Therefore, we had performed an independent study of Sn enthalpy increment [27, 28] and came to the conclusion that the data [22] are the most suitable one for making calorimeter's calibration. Comparison between various reference data on ΔH of Sn at high temperatures [22, 26, 29, 30] and our results [27, 28] is considered in Table 1. One can see that the values reported by Veryatin et al. [30] are evidently overestimated. The values of ΔH taken from [26] and [29] are almost identical. Our experimental points are in a best agreement with the temperature dependence of ΔH [22] being extrapolated up to $1200 \text{ }^\circ\text{C}$.

As it is well known (see, e.g., [25]), the correctness of the calorimeter's calibration is of critical importance for the accurate and reliable calorimetric results. In our case, the determination of the sensitivity calibration factor k of the instrument consisted of two parts. Initially, the samples of the first component of the alloy were successively introduced into the measuring detector for the gradual

Table 1 Experimental values of Sn enthalpy increment in comparison with the reference data

Temperature/°C	$\Delta H/J\text{ g}^{-1}$				
	Our experiment [27, 28]	[22] ^a	[26]	[29]	[30]
549	184.672	186.394	186.212	186.188	192.020
598	194.267	197.505	197.958	197.931	204.640
649	206.109	208.870	210.183	210.154	217.776
698	219.137	219.600	221.929	221.898	230.397
749	234.991	230.570	234.154	234.121	243.532
798	235.176	240.920	245.900	245.865	256.153
849	250.982	251.494	258.125	258.088	269.288
899	263.180	261.665	270.111	270.071	282.166
949	265.367	271.642	282.096	282.055	295.045
1000	277.087	281.618	294.321	294.278	308.180
1049	291.677	291.013	306.067	306.022	320.801
1099	296.921	300.408	318.053	318.005	333.679
1149	314.526	309.609	330.038	329.988	346.557
1202	312.602	319.150	342.743	342.691	360.208

^aExtrapolation of low-temperature (≤ 527 °C) data

accumulation of the first liquid metal in analytical crucible. Taking into account the all-round pattern of heat flux recording in a 3D-type measuring detector, the value of k was postulated to be constant and independent of the number of introduced samples. It was determined as the arithmetic mean for all the drops. After completion of the multiple adding of the second component with the formation of an alloy of approximately equimolar composition, several pieces of a reference sapphire were additionally fed to the liquid metal mirror and the value of k was again calculated. Finally, to measure the mixing enthalpy, we have not used $k = \text{const}$, but assumed a linear change in k with the mass of the melt during the dilution of the alloy with the second component. The application of factor k correction by sapphire samples adding to mixing enthalpy measurement was discussed in detail earlier in [31]. The error of enthalpy determination taking into account possible inaccuracies of experiments and reference data was about $\pm 5\%$.

Results and discussion

Experimental results on heat effects of the binary liquid Ag–Sn alloy formation at 1150 °C are represented in Fig. 1. The experimental data cover the entire compositional range from pure silver to pure tin and lie completely in the negative region of the graph indicating the exothermic nature of interparticle interactions.

The dots show the compositional dependence of the mixing enthalpy ΔH_{mix} at 1150 °C, represented by two

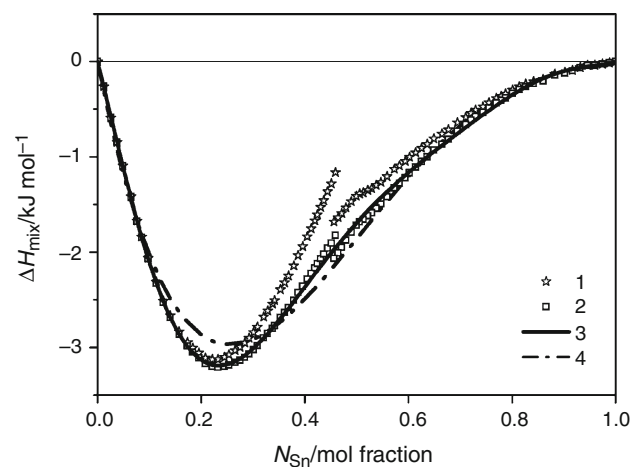


Fig. 1 Compositional dependency of Ag–Sn alloys mixing enthalpy at 1150 °C. 1 Experimental data after the primary calibration using pure components; 2 the same data after additional correction of calibration by leucosapphire samples; 3 approximation of experimental points by Eq. (1); 4 approximation of experimental points by Eq. (3)

opposite branches. The position of the asterisks on the graph was found taking into account the instrument's sensitivity calibration by the first pure components only. It can be seen that such calibration does not give a smooth transition of one branch into another. The squares represent the same results after applying the supplementary calibration by sapphire samples.

Both series of experimental points contain smoothed stepwise segment in the range $0.47 < N_{\text{Sn}} < 0.53$. The nature of this phenomenon is unclear. To our regret, drop

calorimetry alone is not able to explain the mentioned anomaly. An extra study is required. However, it is important to note that the tabulated raw data on Ag–Sn mixing enthalpy at 1250 °C reported in [23] demonstrate the similar behavior around 55–60 at.% Sn being plotted versus composition.

Correction of k by adding sapphire samples significantly improves the convergence of the counter branches of the ΔH_{mix} isotherm, but it does not solve the problem completely. Therefore, two branches of square dots were finally approximated by a common analytic function of the following kind:

$$\Delta H_{\text{mix}} = N_{\text{Ag}} \cdot N_{\text{Sn}} \cdot (a + b \cdot N_{\text{Sn}} + c \cdot N_{\text{Sn}}^2 + d \cdot N_{\text{Sn}}^3 + \dots),$$

where a, b, c, d, \dots are const, and $N_{\text{Ag}}, N_{\text{Sn}}$ are molar fractions of the components.

For this purpose, we reduced the measured points to $\Delta H_{\text{mix}} \cdot N_{\text{Ag}}^{-1} \cdot N_{\text{Sn}}^{-1}$ and described experimental data in Fig. 2 with a power polynomial using the least square method to determine the best degree and coefficients of polynomial. It was found out that the power polynomial should be at least of the fifth order and has the following constant parameters for good approximation of $\Delta H_{\text{mix}} \cdot N_{\text{Ag}}^{-1} \cdot N_{\text{Sn}}^{-1}$ with R -squared coefficient of determination $R^2 = 0.999$:

$$\Delta H_{\text{mix}} = N_{\text{Ag}} \cdot N_{\text{Sn}} \cdot (-22.068 - 60.141 \cdot N_{\text{Sn}} + 577.07 \cdot N_{\text{Sn}}^2 - 1300.6 \cdot N_{\text{Sn}}^3 + 1233.7 \cdot N_{\text{Sn}}^4 - 429.49 \cdot N_{\text{Sn}}^5), \text{ kJ mol}^{-1}. \quad (1)$$

Results of the experimental data fitting with the use of Eq. (1) are represented with a solid line in Figs. 1 and 2. The above-stated approximation is accurate, but it is purely mathematical procedure and has no certain physical meaning.

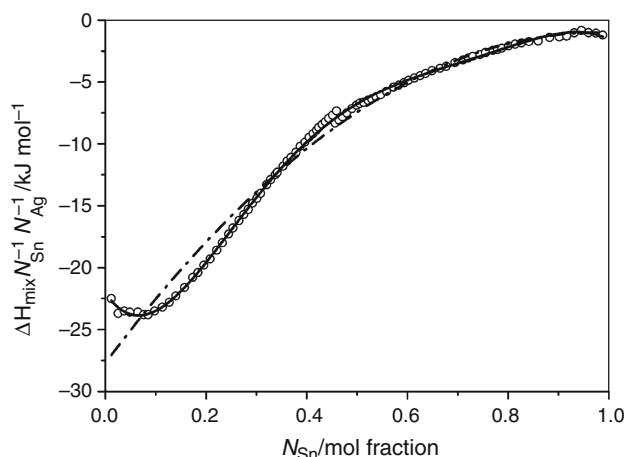


Fig. 2 Approximation of the experimental data on $\Delta H_{\text{mix}}/(N_{\text{Ag}} \cdot N_{\text{Sn}})$ (circles) using Eq. (1) (solid line) and Eq. (3) (dash-and-dot line)

That is why we performed one more approximation using the theory of solutions. Results of the latter fitting are represented in Figs. 1 and 2 with a dash-and-dot line. Owing to the complex shape of the ΔH_{mix} isotherm, a quasi-chemical model of the subregular solutions considering pair and ternary interparticle interactions in the melt was selected to approximate the experimental points. In general, the mixing heat isotherm in this model is described by the equation [32]:

$$\Delta H_{\text{mix}} = N_{\text{Ag}} \cdot N_{\text{Sn}} \cdot (\alpha_1 \cdot N_{\text{Ag}} + \alpha_2 \cdot N_{\text{Sn}} - \alpha_3 \cdot N_{\text{Ag}} \cdot N_{\text{Sn}}), \quad (2)$$

where $\alpha_1, \alpha_2, \alpha_3$ are const.

In order to fit the experimental points by Eq. (2), the values of N_{Ag} in brackets were replaced with $(1 - N_{\text{Sn}})$ giving finally the following equation:

$$\Delta H_{\text{mix}}/(N_{\text{Ag}} \cdot N_{\text{Sn}}) = A + B \cdot N_{\text{Sn}} + C \cdot N_{\text{Sn}}^2,$$

where A, B, C are const and are equal to $\alpha_1, -\alpha_1 + \alpha_2 - \alpha_3$ and α_3 , respectively.

The experimental results taken as $\Delta H_{\text{mix}}/(N_{\text{Ag}} \cdot N_{\text{Sn}})$ were described by a parabolic function using the least square method with the determination of A, B and C values (Fig. 2). The R -squared coefficient of determination was $R^2 = 0.983$. This procedure allowed us to estimate the values of the α coefficients in Eq. (2), which finally acquired the form:

$$\Delta H_{\text{mix}} = N_{\text{Ag}} \cdot N_{\text{Sn}} \cdot (-27.7075 \cdot N_{\text{Ag}} - 0.9977 \cdot N_{\text{Sn}} + 27.7079 \cdot N_{\text{Ag}} \cdot N_{\text{Sn}}), \text{ kJ mol}^{-1}. \quad (3)$$

Both the experimental points and the approximating curve in Fig. 1 have pronounced asymmetry, while the strongest exothermic interparticle interaction being observed at a tin content is about 23%.

In Fig. 3 the integral ΔH_{mix} of Ag–Sn system is shown together with the partial molar mixing enthalpies $\Delta \bar{H}_{\text{mix}}$ of

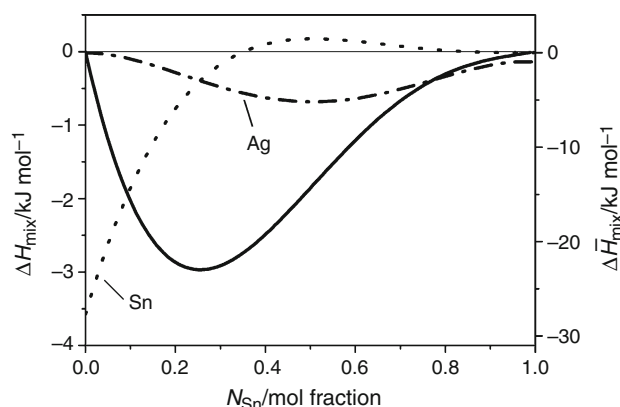


Fig. 3 Enthalpies of components mixing in the Ag–Sn system at 1150 °C. Solid line—integral mixing enthalpy; dot line and dash-and-dot line—partial molar mixing enthalpies

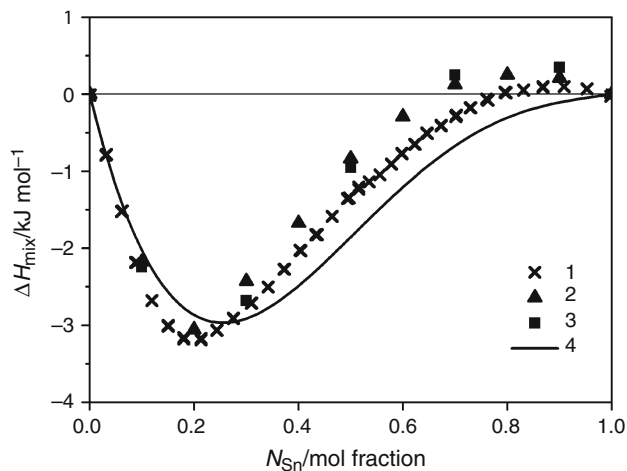


Fig. 4 Ag–Sn mixing enthalpy isotherms by different authors. 1 Data [5] at 1250 °C, 2 data [22] at 1150 °C, 3 data [24] at 1127 °C, 4 our data at 1150 °C

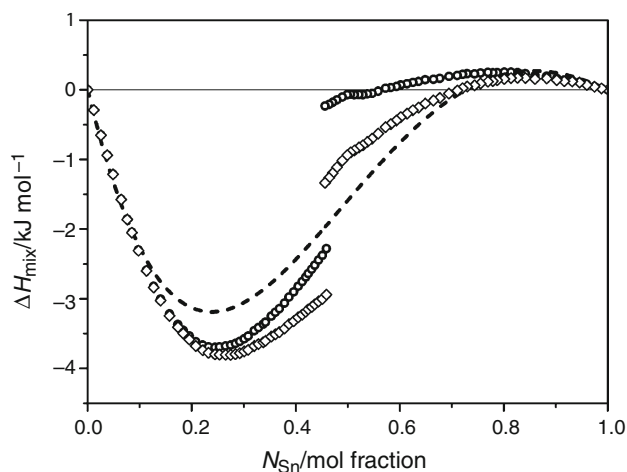


Fig. 5 Reconstruction of Fig. 1 by the application of data [26] on the enthalpy of both pure components to sensitivity calibration of the calorimeter. Circles—experimental data after the primary calibration using pure components; rhomb dots—the same data after additional correction of calibration by leucosapphire samples; dash line—approximation of experimental points by quasi-chemical model of the subregular solutions

components. The partial molar mixing enthalpy of tin is determined using differentiation of Eq. (3) with respect to N_{Sn} , and $\Delta\bar{H}_{\text{mix}}$ of silver was found from the Gibbs–Duhem equation.

Our results are compared with the available information on Ag–Sn ΔH_{mix} [22–24] in Fig. 4. In general, our results do not contradict the known data concerning value and shape of the $\Delta H_{\text{mix}}(N_{\text{Sn}})$ curve. But at a high tin contents our isotherm remains in the negative region, whereas the data of the other authors are slightly positive.

As mentioned above, the reference data on enthalpy increment of pure Sn by Dinsdale [26] seem to be less suitable for heat calibration of the calorimeter in comparison with [22]. Nevertheless, we made an attempt to recalculate experimental data and reproduce Fig. 1 using data [26] for both pure Sn and Ag. Results are given in Fig. 5.

One can see from Fig. 5 that the sensitivity calibration of the calorimeter using the substitution of data [22] on Sn enthalpy increment at 1150 °C with that of [26] makes the shape of ΔH_{mix} curve and its sign closer to the previous data of the other authors. But it does not provide satisfactory convergence of the opposite branches of the isotherm.

Conclusions

It was shown by the experimental study that the obtained ΔH_{mix} isotherm in general does not disagree with the results of other authors, but our curve does not change its sign and lies entirely in the region of exothermic thermal effects. The detected difference may be explained by the fact that previous researchers had used less accurate high-temperature literature data on the enthalpy of tin for calorimeter calibration.

Acknowledgements The work was carried out within the State Assignment (Project No. 0396-2015-0079) using shared equipment of the “Ural-M” center.

References

1. Tian F, Liu ZQ, Shang PJ, Guo J. Phase identification on the intermetallic compound formed between eutectic SnIn solder and single crystalline Cu substrate. *J Alloys Comp.* 2014;591:351–5.
2. Keller J, Baither D, Wilke U, Schmitz G. Mechanical properties of Pb-free SnAg solder joints. *Acta Mater.* 2011;59:2731–41.
3. Herat S. Green electronics through legislation and lead free soldering. *Clean Soil Air Water.* 2008;36:145–51.
4. Cheng S, Huang CM, Pecht M. A review of lead-free solders for electronics applications. *Microelectron Reliab.* 2017;75:77–95.
5. Luef C, Flandorfer H, Ipser H. Lead-free solder materials: experimental enthalpies of mixing in the Ag–Cu–Sn and Cu–Ni–Sn ternary systems. *Zeitschrift für Metallkunde.* 2004;95:151–63.
6. Mouas M, Gasser JG, Hellal S, Grosdidier B. Static structure and dynamic properties in liquid $\text{Sn}_{96.2}\text{Ag}_{3.8}$ lead free solder: structure factor, diffusion coefficients and viscosity. *Calphad.* 2014;44:102–7.
7. Hu X, Li Y, Liu Y, Min Z. Developments of high strength Bi-containing Sn0.7Cu lead-free solder alloys prepared by directional solidification. *J Alloys Comp.* 2015;625:241–50.
8. Yang Y, Balaraju JN, Huang Y, Liu H, Chen Z. Interface reaction between an electroless Ni–Co–P metallization and Sn-3.5Ag lead-free solder with improved joint reliability. *Acta Mater.* 2014;71:69–79.

9. Nazeri MFM, Ismail AB, Mohamad AA. Effect of polarizations on Sn-Zn solders alloys in alkaline electrolyte. *J Alloys Comp.* 2014;606:278–87.
10. Öztürk E, Aksöz S, Altuntas Y, Keşlioğlu K, Maraşlı N. Experimental measurements of some thermophysical properties of solid CdSb intermetallic in the Sn–Cd–Sb ternary alloy. *J Therm Anal Calorim.* 2016;126:1059–65.
11. Wang F, Zhou L, Zhang Z, Wang J, Wang X, Wu M. Effect of Sn–Ag–Cu on the improvement of electromigration behavior in Sn-58Bi solder joint. *J Electron Mater.* 2017. <https://doi.org/10.1007/s11664-017-5655-x>.
12. Kotadia HR, Howes PD, Mannan SH. A review: on the development of low melting temperature Pb-free solders. *Microelectron Reliab.* 2014;54:1253–73.
13. Amin NAAM, Shnawah DA, Said SM, Sabri MFM, Arof H. Effect of Ag content and the minor alloying element Fe on the electrical resistivity of Sn–Ag–Cu solder alloy. *J Alloys Comp.* 2014;599:114–20.
14. Ho CY, Tsai MT, Duh JG, Lee JW. Bump height confinement governed solder alloy hardening in Cu/SnAg/Ni and Cu/SnAgCu/Ni joint assemblies. *J Alloys Comp.* 2014;600:199–203.
15. Huang ML, Zhao N, Liu S, He YQ. Drop failure modes of Sn–3.0Ag–0.5Cu solder joints in wafer level chip scale package. *Trans Nonferrous Metals Soc China.* 2016;26:1663–9.
16. Shnawah DA, Said SBM, Sabri MFM, Badruddin IA, Che FX. High-reliability low-Ag-content Sn–Ag–Cu solder joints for electronics applications. *J Electron Mater.* 2012;41:2631–58.
17. Giuranno D, Delsante S, Borzone G, Novakovic R. Effects of Sb addition on the properties of Sn–Ag–Cu/(Cu, Ni) solder systems. *J Alloys Comp.* 2016;689:918–30.
18. Drienovsky M, Rizekova Trnkova L, Ozvold M, Cernickova I, Palcut M, Janovec J. Melting behavior and oxidation resistance of Ce–Sn alloy designed for lead-free solder manufacturing. *J Therm Anal Calorim.* 2016;125:1009–15.
19. Li Z, Dallegri M, Knott S. Calorimetric measurements of the ternary Ag–Au–Sn system. *J Alloys Comp.* 2008;453:442–7.
20. Xu S, Chan YC, Zhang K, Yung KC. Interfacial intermetallic growth and mechanical properties of carbon nanotubes reinforced Sn3.5Ag0.5Cu solder joint under current stressing. *J Alloys Comp.* 2014;595:92–102.
21. Khodabakhshi F, Sayyadi R, Shahamat Javid N. Lead free Sn–Ag–Cu solders reinforced by Ni-coated graphene nanosheets prepared by mechanical alloying: microstructural evolution and mechanical durability. *Mater Sci Eng A.* 2017;702:371–85.
22. Kubaschewski O, Alcock CB. *Metallurgical thermochemistry.* Moscow: Metallurgia; 1982 (in Rus).
23. Flandorfer H, Luef C, Saeed U. On the temperature dependence of the enthalpies of mixing in liquid binary (Ag, Cu, Ni)–Sn alloys. *J Non Cryst Solids.* 2008;354:2953–72.
24. Hultgren RR, Orr L, Anderson PD, Kelley KK. *Selected values of thermodynamic properties of metals and alloys.* New York: Wiley; 1963.
25. Pool MJ, Predel B, Schultheiss E. Application of the Setaram high temperature calorimeter for the determination of mixing enthalpies of liquid alloys. *Thermochim Acta.* 1979;28:349–58.
26. Dinsdale AT. *SGTE data for pure elements.* Calphad. 1991;15:317–425.
27. Oleinik KI, Bykov AS, Pastukhov EA. Enthalpy increment of liquid tin under high overheating. In: XX Mendeleev congress on general and applied chemistry, 26–30 September 2016, Ekaterinburg, Russia. Section 3—Physical chemistry of metallurgical processes. Vol. 3: abstracts. Ekaterinburg: Ural Branch of the Russian Academy of Sciences, 2016, p. 179.
28. Oleinik KI, Bykov AS, Pastukhov EA. Clarification of liquid tin thermal properties at high temperatures. *Raspilavy.* 2017;5:398–403 (in Rus).
29. Barin I. *Thermochemical properties of pure substances.* VCh, 1993, in 2 parts.
30. Veryatin UD, Mashirev VP, Ryabtsev NG, Tarasov VI, Rogozkin BD, Korobov IV. *Thermodynamic properties of inorganic substances.* Moscow: Atomizdat; 1965 (in Rus).
31. Filippov VV, Bykov AS, Pastukhov EA. New method of calibration for the determination of mixing enthalpies of liquid alloys in drop calorimetry. *Russ Metallurgy (Metally).* 2014;2014:81–4.
32. Sharkey RL, Pool MJ, Hoch M. Thermodynamic modeling of binary and ternary metallic solutions. *Met Mater Trans B.* 1971;2:3039–49.